Available online at www.sciencedirect.com
ScienceDirect
Journal of Hazardous Materials 152 (2008) 778–788
Journal of Hazardous Materials
www.elsevier.com/locate/jhazmat

Investigation of nickel(II) biosorption on *Enteromorpha prolifera*: Optimization using response surface analysis

Ayla Özer [a,*], Görkem Gürbüz [a], Ayla Çalimli [b], Bahadır K. Körbahti [a]

[a] *Mersin University, Chemical Engineering Department, 33343 Çiftlikköy-Mersin, Turkey*
[b] *Ankara University, Chemical Engineering Department, Tandoğan-Ankara, Turkey*

Received 13 April 2007; received in revised form 17 July 2007; accepted 17 July 2007
Available online 31 July 2007

Abstract

In this study, the biosorption of nickel(II) ions on *Enteromorpha prolifera*, a green algae, was investigated in a batch system. The single and combined effects of operating parameters such as initial pH, temperature, initial metal ion concentration and biosorbent concentration on the biosorption of nickel(II) ions on *E. prolifera* were analyzed using response surface methodology (RSM). The optimum biosorption conditions were determined as initial pH 4.3, temperature 27 °C, biosorbent concentration 1.2 g/L and initial nickel(II) ion concentration 100 mg/L. At optimum biosorption conditions, the biosorption capacity of *E. prolifera* for nickel(II) ions was found to be 36.8 mg/g after 120 min biosorption. The Langmuir and Freundlich isotherm models were applied to the equilibrium data and defined very well both isotherm models. The monolayer coverage capacity of *E. prolifera* for nickel(II) ions was found as 65.7 mg/g. In order to examine the rate limiting step of nickel(II) biosorption, such as the mass transfer and chemical reaction kinetics, the intraparticle diffusion model, external diffusion model and the pseudo second order kinetic model were tested with the experimental data. It was found that for both contributes to the actual biosorption process. The pseudo second order kinetic model described the nickel(II) biosorption process with a good fitting.

Keywords: Response surface methodology (RSM); Nickel(II); *Enteromorpha prolifera*; Biosorption

1. Introduction

The primary sources of nickel wastes are the plating and metal-processing industries. Nickel(II) may be found in wastewater discharges from mine drainage, dye house effluent, paint and ink formulation, electroplating, and porcelain enameling activities, battery and accumulator manufacturing. High levels of nickel have also been reported in wastes from silver refineries. In addition, basic steel works and foundries, motor vehicle and aircraft industries, and printing are potential sources of nickel [1]. Nickel is toxic to a variety of aquatic organisms, even at very low concentration [2].

Nickel exists in waste streams predominantly as the soluble ion. In the presence of complexing agents such as ammonia, EDTA, or cyanide, nickel may exist in a stable soluble form. The formation of nickel–cyanide complexes interferes with both cyanide and nickel treatment, and the presence of this species may be responsible for high levels of both cyanide and nickel in treated wastewater effluents [1].

Conventional treatment technologies such as precipitation, ion exchange and adsorption have been employed to remove nickel(II) ions from aqueous solution [2]. These conventional techniques can reduce metal ions, but they do not appear to be highly effective due to the limitations in the pH range as well as the high material and operational costs [3]. The most popular of these technologies is activated carbon adsorption and widely used but it is expensive. Therefore, there is a growing interest in using low-cost, easily available materials for the adsorption of metal ions. A low-cost adsorbent is defined as one which is abundant in nature, or is a by-product or waste material from another industry. Biosorbent materials derived from suitable biomass can be used for the effective removal and recovery of heavy metal ions from industrial solutions. Many algae, yeasts, bacteria and other fungi are known to be capable of concentrating metal species from dilute aqueous solutions and accumulating them within their cell structure. Microorganisms are known to accu-

* Corresponding author. Fax: +90 324 3610032.
E-mail address: ayozer@mersin.edu.tr (A. Özer).

0304-3894/$ – see front matter © 2007 Elsevier B.V. All rights reserved.
doi:10.1016/j.jhazmat.2007.07.088

Nomenclature

b	constant related to the affinity of the binding sites (L/mg)
C	metal ion concentration at any time t (mg/L)
C_{eq}	metal ion concentration remaining in solution at equilibrium (mg/L)
C_o	initial metal ion concentration (mg/L)
e_i	error in the model, $i = 1–4$
k_2	pseudo second order rate constant (g/mg min)
K_F	adsorption capacity
K_i	intraparticle diffusion rate constant (mg/g $min^{1/2}$)
n_F	biosorption intensity
q	amount of biosorbed metal on the surface of the biosorbent at any time t (mg/g)
q_{eq}	the amount of biosorbed metal per unit weight of biosorbent at equilibrium (mg/g)
$q_{eq,cal}$	calculated amount of biosorbed metal per unit weight of biosorbent at equilibrium (mg/g) from the pseudo second order kinetic model
$q_{eq,exp}$	experimental amount of biosorbed metal per unit weight of biosorbent at equilibrium (mg/g)
q_f	amount of biosorbed metal on the surface of the biosorbent at the end of biosorption (mg/g)
q_{max}	maximum monolayer coverage capacity of biosorbent (mg/g)
R^2	correlation coefficient
R^2_{adj}	adjusted correlation coefficient
S	specific surface area (m^2/g biosorbent)
t	time (min)
x_i	independent variable, $i = 1–4$
X_o	biosorbent concentration (g/L)
y_i	response, $i = 1–4$

Greek letters

β_o, β_i and β_{ij}	linear and quadratic interaction coefficients, i and $j = 1–4$
β_L	external diffusion constant (cm/min)
η	response

mulate metals by two distinct processes: (i) bioaccumulation, an energy-dependent process, and (ii) biosorption, an energy independent physical adsorption [4]. Biosorption of heavy metal ions to biosorbent is affected by several factors including the specific surface properties of the microorganisms and the physicochemical properties of the solution. Cell walls of organisms possess various mechanisms for metal biosorption such as complexation, coordination, chelation, ion exchange, inorganic precipitation and/or a combination of these [5]. The major advantages of the biosorption technology are its effectiveness in reducing the concentration of heavy metal ions to very low levels and the use of inexpensive biosorbent materials [6].

Many workers have reported the potential of marine algae otherwise known as seaweeds for biosorption of heavy metal ions [6–11]. However, the applicability of *Enteromorpha prolifera*, a green seaweed, for nickel(II) biosorption has not been reported in literature. Seaweeds are a widely available source of biomass as over two million tonnes are either harvested from the oceans or cultured annually for food or phycocolloid production [12].

The purpose of this study was to investigate the biosorption characteristics of nickel(II) ions on *E. prolifera*. The effects of operating parameters such as initial pH, temperature, initial metal ion and biosorbent concentrations were optimized using response surface methodology (RSM). The optimization of experimental conditions using RSM was widely applied in various processes, however, its application in biosorption processes is very rare. The equilibrium and kinetic models were also applied to the experimental data using various models.

2. Material and methods

2.1. Preparation of biosorbent

E. prolifera, a kind of green algae, was obtained from Mediterranean costs in Mersin, Turkey. The algae was washed twice with tap water in order to remove dirties. It was dried in sunlight for 1–2 days and then in an oven at 105 °C for 24 h until all the moisture evaporated, put in distilled water and blended by using a commercial blender (Waring) to obtain larger surface area. A stock solution of 10 g/L of biosorbent was prepared.

2.2. Nickel(II) solution

A stock solution of nickel (II) (1.0 g/L) was prepared by dissolving weighed amount of $NiCl_2$ in 1 L of distilled water. Necessary dilutions were made from the stock solution to prepare solutions in the range of concentrations 25–300 mg/L. The initial pH of each solution was adjusted to the required value with 1 and 0.1 M HCl and NaOH solutions before mixing the biosorbent suspension.

2.3. Batch biosorption studies

Batch biosorption experiments were performed in 250 mL Erlenmeyer flasks containing 100 mL of biosorption solution. For this, 10 mL of biosorbent suspension, except for the biosorbent concentration experiments, was mixed with 90 mL of the metal bearing solution of known initial nickel(II) concentration and initial pH and then the flasks were agitated on a shaker at 100 rpm for 2 h, which is more than ample time for biosorption equilibrium. Samples were taken before mixing the biosorbent suspension and nickel bearing solution and at predetermined time intervals. Samples were filtered by using filter paper and the nickel(II) ion concentration remaining in supernatant was analysed. For isotherm experiments, the initial nickel(II) ion concentrations were varied while the biosorbent concentration in each sample was held constant at 1.0 g/L.

2.4. Nickel(II) Analysis

The concentration of nickel(II) ion remaining in the biosorption medium was determined spectrophotometrically. 0.2 mL of 1% (w/v) sodium diethyl dithiocarbamate solution, and 20 mL of 1.5 N NH_3 solution were added to the sample (1 mL) containing lower than 5–40 mg/L of nickel(II) ions and diluted to 25 mL with distilled water. The absorbance of the colored solution was read at 340 nm. The biosorbed metal amount (mg/g) and biosorption percent (%) at any time, t, were computed as follows, respectively:

$$q(\text{mg/g}) = (C_o - C)/X_o \quad (1)$$

$$\text{Biosorption percent}(\%) = \left[\frac{C_o - C}{C_o}\right] \times 100 \quad (2)$$

where C_o and C (mg/L) are the metal ion concentration at initial time $t = 0$ and any time t (min), respectively and X_o is the biosorbent concentration (g/L).

2.5. Experimental design and optimization

In the study, the effects of operating parameters were optimized using response surface methodology (RSM). RSM is essentially a particular set of mathematical and statistical methods for designing experiments, building models, evaluating the effects of variables, and searching optimum conditions of variables to predict targeted responses. It is an important branch of experimental design and a critical technology in developing new processes, optimizing their performance, and improving design and formulation of new products. Its greatest applications particularly have been in situations where a large number of variables influencing the system feature. This feature termed as the response and normally measured on a continuous scale, which represents the most important function of the systems [13,14].

The researcher is often interested in finding a suitable approximating function for the purpose of predicting and determining the future response. Response surface procedures are not primarily used for the purpose of allowing the researcher in order to understand the mechanism of the system or process; rather its purpose is to determine the optimum operating conditions or to determine a region for the factors at a certain operating specifications are met [13,14]. The application of statistical experimental design techniques in sorption processes could result in improved product yields, reduced process variability, closer confirmation of the output response to nominal and targeted requirements, as well as reduced development time and overall costs [15].

In the study, central composite design (CCD) was used for the RSM in the experimental design, which is well suited for fitting a quadratic surface and usually works well for the process optimization. The CCD is an effective design that is ideal for sequential experimentation and allows a reasonable amount of information for testing lack of fit while not involving an unusually large number of design points [13,14].

The CCD consisted of a 2^k factorial runs with $2k$ axial runs and r center runs (three replicates). For each categorical variable, a 2^4 full factorial central composite design for four factor designed experiments consists 16 factorial points, 8 axial points and 3 replicates at the center points, indicating that 27 experiments were augmented and were carried in randomized order as required in many design procedures. The center points were used to evaluate the experimental error and the reproducibility of the data. The independent variables were coded to the (−1, 1) interval where the low and high levels were coded as −1 and +1, respectively. The axial points were located at ($\pm\alpha$, 0, 0), (0, $\pm\alpha$, 0) and (0, 0, $\pm\alpha$) where α is the distance of the axial point from center and makes the design rotatable. In the study, α was fixed 1.0.

Therefore, face centered central composite design with four factors was applied using Design-Expert 6 with the bounds of the factors of initial nickel(II) concentration: 50–150 mg/L, biosorbent concentration: 0.5–2.0 g/L, initial pH 3.0–5.0 and temperature: 20–30 °C as shown in Table 1.

Performance of the process was evaluated by analyzing the response of biosorbent for nickel(II) ions. The responses were biosorption capacity ($\hat{y}_1$) and biosorption percent of biosorbent ($\hat{y}_2$) for nickel(II) ions. The biosorption capacity and biosorption percent values of *E. prolifera* were determined at the end of 120 min biosorption time and they were named as "final".

In the optimization process, the responses can be simply related to chosen factors by linear or quadratic models. A quadratic model, which also includes the linear model, is given as;

$$\eta = \beta_0 + \sum_{j=1}^{k}\beta_j x_j + \sum_{j=1}^{k}\beta_{jj}x_j^2 + \sum_{i}\sum_{<j=2}^{k}\beta_{ij}x_i x_j + e_i \quad (3)$$

The success of the RSM depends on the approximation of η by a low order polynomial in some region of the independent variables. In Eq. (3), η is the response, x_i and x_j are variables, β_o is the constant coefficient, β_j's, β_{jj}'s and β_{ij}'s are interaction coefficients of linear, quadratic and the second order terms, respectively, and e_i is the error. In the study, the biosorption capacities and biosorption percents of biosorbent for nickel(II) ions were processed for Eq. (3) including ANOVA to obtain the interaction between the process variables and the responses. The quality of the fit of polynomial model was expressed by the coefficient of determination R^2 and R^2_{adj}. The statistical significance was checked with adequate precision ratio and F-test.

Table 1
Experimental design of the biosorption of nickel(II) ions on *Enteromorpha prolifera*

Independent variable	Coded levels	
	−1	+1
Initial nickel(II) ion concentration (mg/L)	50	150
Biosorbent concentration (g/L)	0.5	2.0
Initial pH	3.0	5.0
Temperature (°C)	20	30

Table 2
ANOVA results of the quadratic models according to biosorption capacity and biosorption percent of the biosorbent for nickel(II) ions

	Source	Sum of squares	Degrees of freedom	Mean square	*F*-value	Prob > *F*
Final biosorption capacity	Model	5364.66	14	383.19	58.20	<0.0001 significant
	Residual	65.84	10	6.58		
	$R^2 = 0.99$; $R^2_{adj} = 0.97$, adequate precision = 20.17					
Biosorption percent (%)	Model	17243.98	14	1231.71	105.58	<0.0001 significant
	Residual	116.66	10	11.67		
	$R^2 = 0.99$; $R^2_{adj} = 0.98$, adequate precision = 31.80					

3. Results and discussion

3.1. The optimization of biosorption conditions

In the study, the effects of operating variables such as initial nickel(II) ion concentration, biosorbent concentration, temperature and initial pH on the biosorption capacity and biosorption percent of biosorbent for nickel(II) ions were investigated using response surface methodology according to central composite design (CCD), and the initial pH and temperature were selected in order to achieve optimal biosorption capacity and biosorption percent of biosorbent for nickel(II) ions at the end of 120 min of biosorption time.

The batch runs were conducted in CCD designed experiments to visualize the effects of independent factors on responses and the results along with the experimental conditions. The experimental results were evaluated and approximating functions of biosorption capacity and biosorption percent of biosorbent for nickel(II) ions were obtained in Eqs. (4) and (5), respectively.

$$\hat{y}_1 = -31.954 - 9.585 \times 10^{-2}x_1 + 48.447x_2 + 0.589x_3 + 14.061x_4 + 4.312 \times 10^{-2}x_1x_2 - 1.250 \times 10^{-4}x_1x_3 + 1.875 \times 10^{-3}x_1x_4 + 8.125 \times 10^{-2}x_2x_3 + 0.656x_2x_4 - 6.250 \times 10^{-3}x_3x_4 + 5.056 \times 10^{-4}x_1^2 - 22.986x_2^2 - 9.435 \times 10^{-3}x_3^2 - 1.736x_4^2 \quad (4)$$

$$\hat{y}_2 = -68.976 - 0.535x_1 + 57.822x_2 + 3.355x_3 + 25.287x_4 - 0.188x_1x_2 - 2.500 \times 10^{-3}x_1x_3 - 1.250 \times 10^{-2}x_1x_4 + 0.225x_2x_3 + 1.625x_2x_4 + 2.500 \times 10^{-2}x_3x_4 + 3.172 \times 10^{-3}x_1^2 - 12.071x_2^2 - 6.282 \times 10^{-2}x_3^2 - 3.071x_4^2 \quad (5)$$

In Eqs. (4) and (5), $\hat{y}$'s are the responses of biosorption capacity in (mg/g), and biosorption percent of biosorbent for nickel(II) ions at the end of 120 min of biosorption time, respectively. x_1, x_2, x_3 and x_4 are corresponding to independent variables of initial nickel(II) ion concentration (mg/L), biosorbent concentration (g/L), temperature (°C) and initial pH, respectively. ANOVA results of these quadratic models presented in Table 2 indicating that these quadratic models can be used to navigate the design space. As can be seen in Table 2, the model *F*-values for the biosorption capacity and biosorption percent of biosorbent for nickel(II) ions were evaluated as 58.20 and 105.58, respectively. These values indicated that the quadratic models were significant. Adequate precision measures the signal to noise ratio and a ratio greater than 4 is desirable. Therefore, in the quadratic models of biosorption capacity and biosorption percent for nickel(II) ions, the ratios of 20.17 and 31.80 indicate adequate signals for the models to be used to navigate the design space. As a result, these quadratic functions could be used for the purpose of predicting future responses successfully for nickel(II) biosorption on *E. prolifera*.

In order to determine the optimal pair temperature and pH to achieve both good biosorption capacity and biosorption percent of biosorbent for nickel(II) ions, Eqs. (4) and (5) have been used to visualize the effects of experimental factors on responses in Figs. 1–7.

The normal probability and studentized residuals plot is shown in Fig. 1 for the biosorption capacity and biosorption percent of biosorbent for nickel(II) ions. In Fig. 1, residuals show how well the model satisfies the assumptions of the analysis of variance (ANOVA) where the studentized residuals measure the number of standard deviations separating the actual and predicted values. Fig. 1 shows that neither response transformation needed nor there was apparent problem with normality.

The actual and the predicted biosorption capacity and biosorption percent plots of biosorbent for nickel(II) ions are shown in Fig. 2. Actual values are the measured response data for a particular run, and the predicted values are evaluated using the approximating functions generated for the models. In Fig. 2a, the values of R^2 and R^2_{adj} were evaluated as 0.99 and 0.97 for nickel(II) biosorption capacity, and in Fig. 2b were determined as 0.99 and 0.98 for nickel(II) biosorption at the end of 120 min. The correlation coefficients showed that the predicted responses very well fit the calculated biosorption capacity and biosorption percent of *E. prolifera* at the end of the biosorption for nickel(II) ions.

The effect of initial pH and temperature on biosorption capacity for nickel(II) ions is shown in Fig. 3 as a semispherical response surface plot. The biosorption capacity of *E. prolifera* increased up to pH 4.3 and above this value decreased with the increase in pH. The biosorption capacity of *E. prolifera* increased with the increase in biosorption temperature up to 27 °C and did not change significantly above this temperature value. An optimum point of maximum biosorption capacity obtained as 36.8 mg/g at 27 °C, pH 4.3, 100 mg/L initial nickel(II) ion concentration and 1.2 g/L biosorbent concentration.

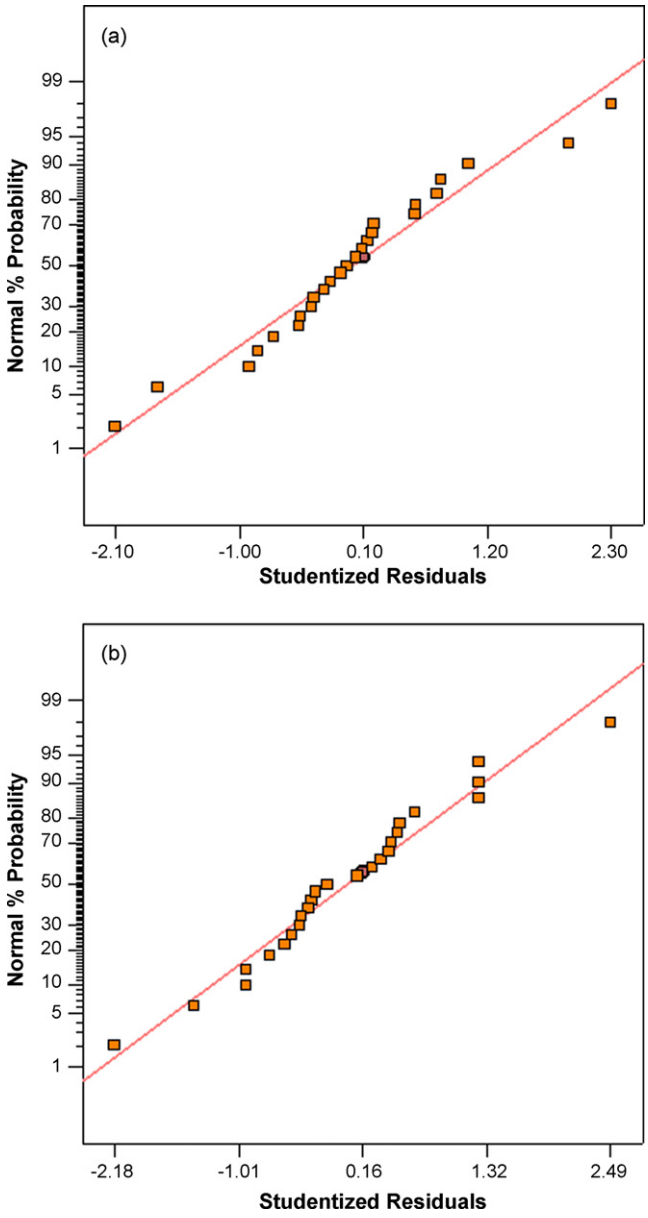

Fig. 1. The studentized residuals and normal% probability plot for the biosorption of nickel(II) ions.

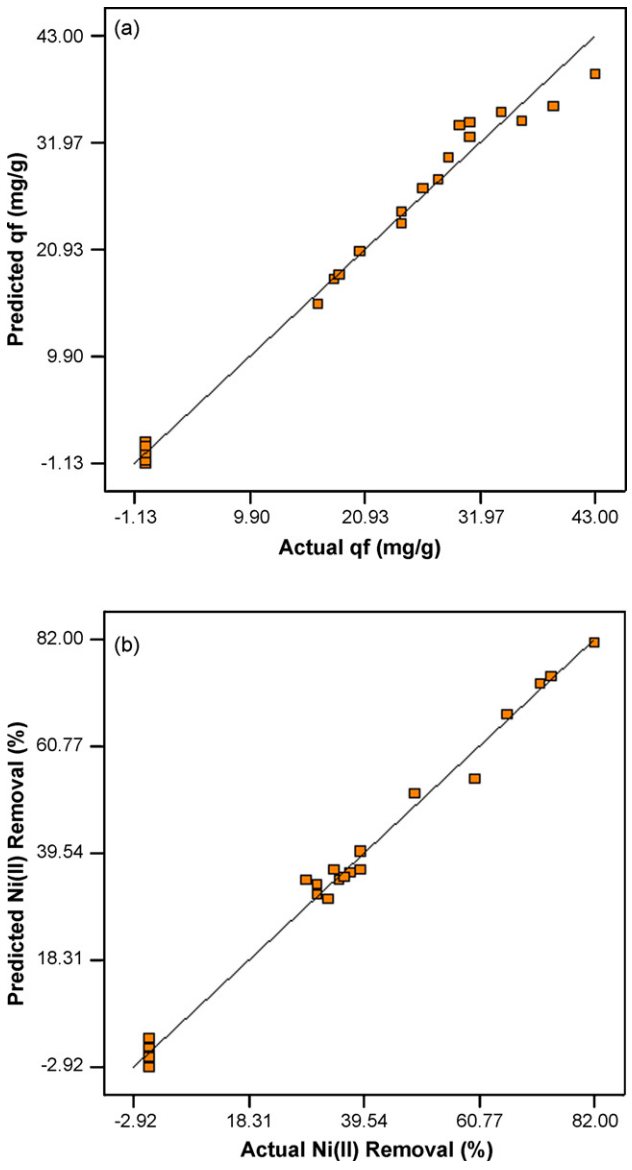

Fig. 2. The actual and predicted plot for nickel(II) biosorption.

Fig. 4 shows the effect of initial nickel(II) and biosorbent concentration on biosorption capacity of *E. prolifera*. In Fig. 4, the maximum biosorption capacity determined at 1.2 g/L biosorbent concentration. Biosorption capacity of *E. prolifera* increased from 23.9 to 36.8 mg/g when the biosorbent concentration increases from 0.5 to 1.2 g/L for the nickel(II) concentration of 100 mg/L at initial pH 4.3 and 27 °C.

In the perturbation plot (Fig. 5) the effects of all the factors at the optimal run conditions in the design space are compared. The plot was obtained at 100 mg/L initial nickel(II) ion concentration, 1.2 g/L biosorbent concentration, 27 °C temperature and initial pH 4.3. In Fig. 5, a steep curvature in biosorbent concentration factor shows that the response of biosorption capacity is very sensitive to this factor. The relatively flat lines of initial nickel(II) ion concentration, temperature and initial pH show insensitivity to change in those particular factors.

In Figs. 6 and 7, the factor interaction plots of $C_o - X_o$, $C_o - T$ and C_o-initial pH on nickel(II) ion uptake capacity of biosorbent and biosorption percent with least significant difference (LSD) bars at the end points of each line on the graphs are shown. An interaction occurs when the response is different depending on the settings of two factors. The LSD bars represent the 95% confidence interval for that particular average value. In Figs. 6 and 7, interactions appear with two non-parallel lines of 50 and 150 mg/L initial nickel(II) concentrations, indicating that the effect of one factor depends on the level of the other. At 150 mg/L initial nickel(II) concentration, nickel(II) biosorption capacities of biosorbent obtained higher than at 50 mg/L for all factors as shown in Fig. 6. In Fig. 7, higher nickel(II) removal percent was obtained at 50 mg/L for all factors. An increase in the initial nickel(II) ion concentration led to an increase in the biosorbed nickel(II) amount on *E. prolifera*. This may be attributed to an increase in the driving force of the concentration gradient with the increase in the initial nickel(II) concentration.

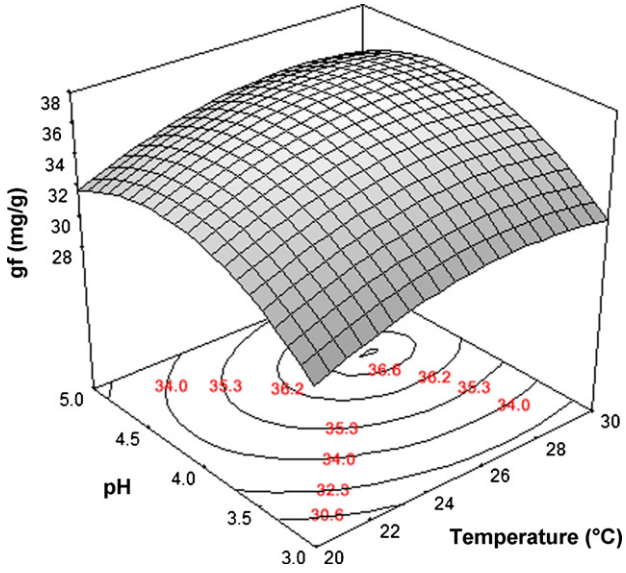

Fig. 3. The combined effect of temperature and initial pH on nickel(II) biosorption (X_o: 1.0 g/L; C_o: 100 mg/L Cu(II); biosorption time: 120 min; agitation rate 100 rpm).

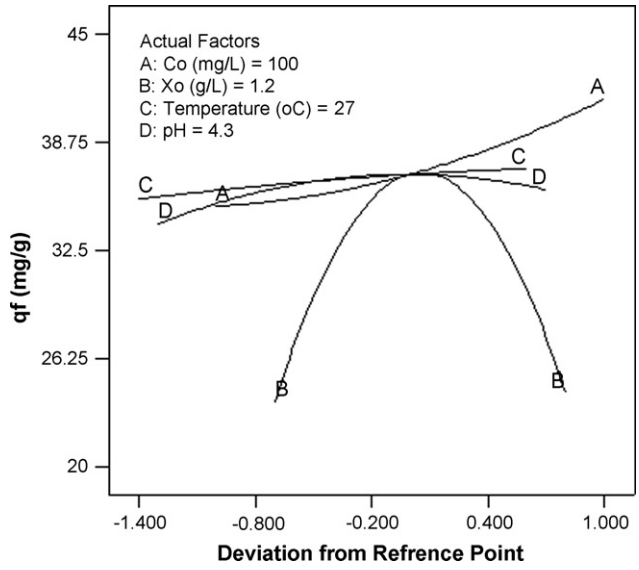

Fig. 5. Perturbation plot for nickel(II) biosorption.

In Fig. 6a, the biosorption capacity of *E. prolifera* increased sharply with increasing biosorbent concentration up to 1.2 g/L and then decreased above 1.2 g/L both at 50 and 150 mg/L initial nickel(II) concentrations. The decrease in nickel(II) biosorption capacity of *E. prolifera* with increasing biosorbent concentration is mainly due to unsaturation of biosorption sites through the biosorption reaction. Another reason may be due to the particle interaction, such as aggregation, resulted from high biosorbent concentration. Such aggregation would be lead to decrease in total surface area of the biosorbent and an increase in diffusional path length [16]. However, nickel(II) removal percent gradually increased with increasing *E. prolifera* concentration as shown in Fig. 7a. Figs. 6b and 7b show that the biosorption capacity and removal percent of *E. prolifera* for nickel(II) ions increased with increasing temperature at initial pH 4.3 with 1.2 g/L biosorbent concentration. In Figs. 6c and 7c, the biosorption capacity and removal percent increased with increasing initial pH up to 4.3 at 27 °C temperature with 1.2 g/L biosorbent concentration. At pH 4.3 and 27 °C biosorption temperature maximum biosorbent uptake capacity was obtained as 35.1 mg/g and 41.2 g/g with 50 and 150 mg/L nickel(II) concentrations, respectively.

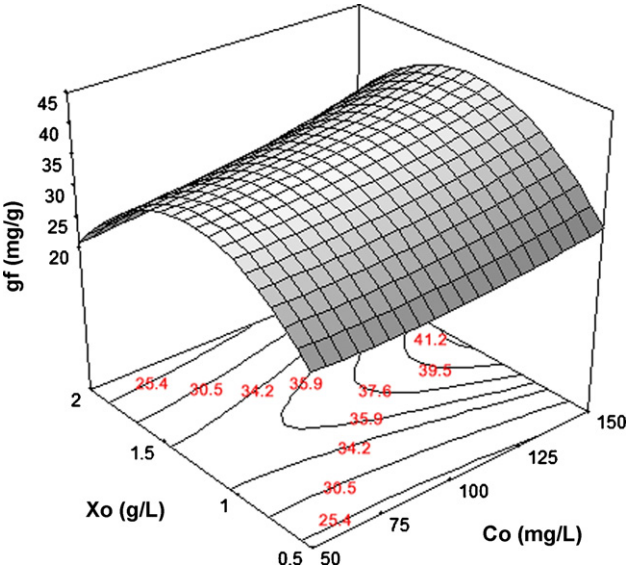

Fig. 4. The combined effect of biosorbent and initial nickel(II) ion concentration on nickel(II) biosorption (T: 27 °C; pH 4.3; biosorption time: 120 min; agitation rate 100 rpm).

3.2. Modeling of the equilibrium

Equilibrium data, commonly known as adsorption isotherms, are basic requirements for the design of adsorption systems [17]. Adsorption isotherms describe how adsorbates interact with adsorbents and are critical in optimizing the use of adsorbents [18]. In order to optimize the design of a adsorption system to remove metal ion from waste streams, it is important to establish the most appropriate correlation for the equilibrium curve.

During biosorption, a rapid equilibrium is established between adsorbed nickel(II) ions on the algal cells (q_{eq}) and unadsorbed nickel(II) ions in solution (C_{eq}). This equilibrium can be represented by the Langmuir and Freundlich isotherm models. The most widely used isotherm equation for modeling equilibrium is the Langmuir equation, based on the assumption that there is a finite number of binding sites which are homogeneously distributed over the adsorbent surface, these binding sites have the same affinity for adsorption of a single molecular layer and there is no interaction between adsorbed molecules [19]. The linearized Langmuir isotherm model is given by Eq. (6);

$$\frac{1}{q_{eq}} = \left[\frac{1}{bq_{max}} \times \frac{1}{C_{eq}}\right] + \frac{1}{q_{max}} \quad (6)$$

where q_{eq} (mg/g) and C_{eq} (mg/L) are the amount of adsorbed dye per unit weight of adsorbent and unadsorbed dye concentration in solution at equilibrium, respectively. q_{max} is the maximum

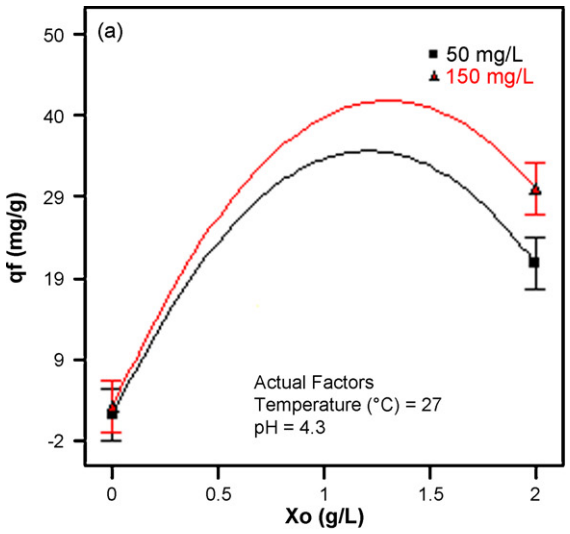

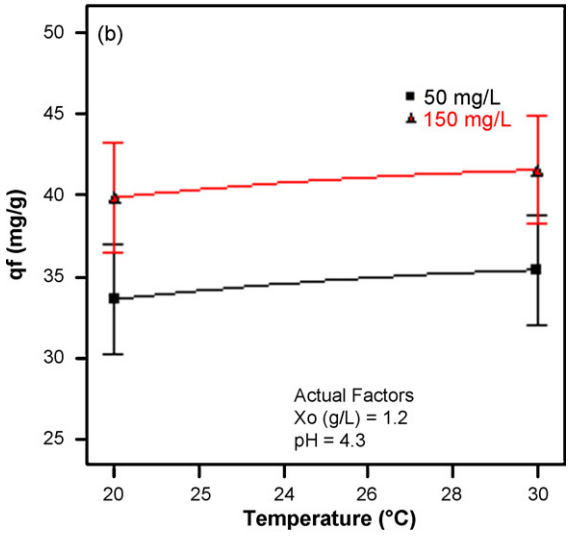

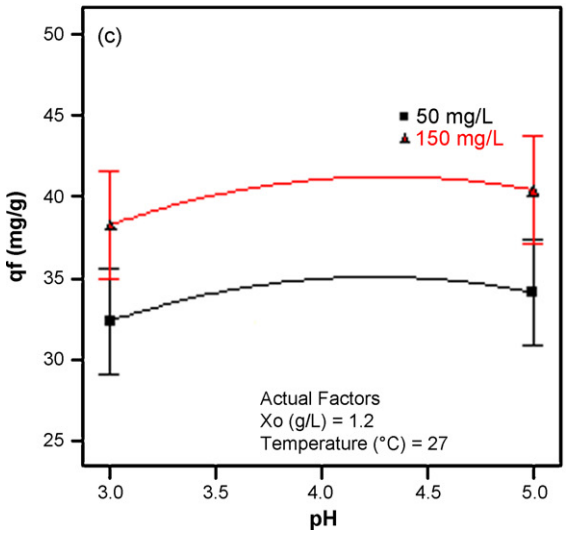

Fig. 6. Two-factor interaction plots for biosorption capacity.

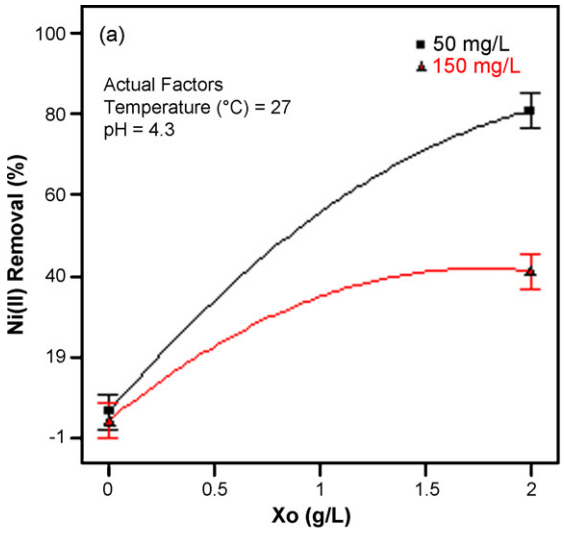

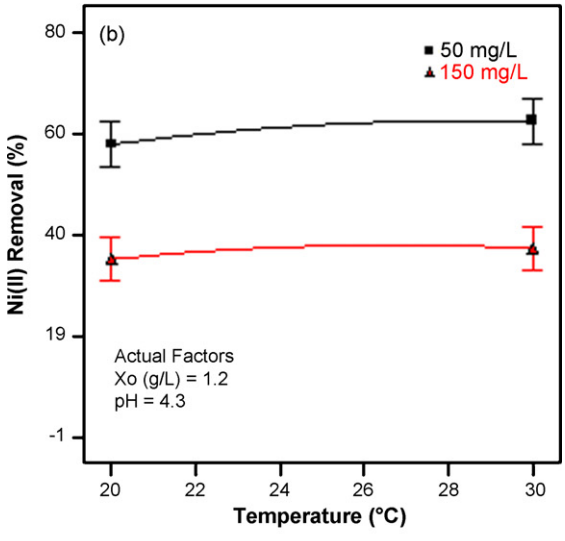

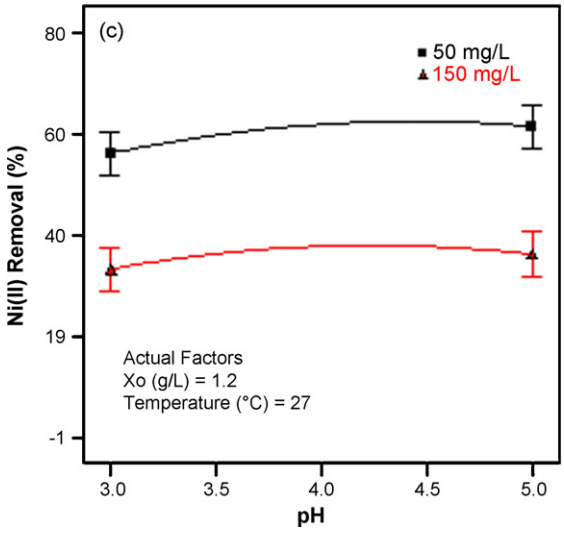

Fig. 7. Two-factor interaction plots for biosorption percent.

amount of the metal per unit weight of adsorbent to form a complete monolayer on the surface bound at high C_{eq} (mg/L) and b (L/mg) represents the affinity constant between the biosorbent and metal ion. q_{max} represents a practical limiting adsorption capacity when the surface is fully covered with dye molecules and it assists in the comparison of adsorption performance, particularly in cases where the adsorbent did not reach its full saturation in experiments.

The Freundlich isotherm is the earliest known relationship describing the adsorption equation [20]. The Freundlich isotherm model is an exponential equation and therefore, assumes that as the adsorbate concentration increases, the concentration of adsorbate on the adsorbent surface also increases. Theoretically using this expression, an infinite amount of adsorption can occur [21]:

$$q_{eq} = K_F C_{eq}^{1/nF} \quad (7)$$

In this equation, K_F and $1/n_F$ are the Freundlich constants indicating adsorption capacity and intensity, respectively.

The Langmuir and Freundlich isotherm models were applied to experimental equilibrium data of nickel(II) biosorption on *E. prolifera* at different temperatures and initial pH values and the isotherm constants were presented in Table 3. As can be seen from Table 3, the monolayer coverage capacity of *E. prolifera* for nickel(II) ions was obtained as 65.36 mg/g at optimum biosorption temperature, 30 °C and initial pH, 5.0. The experimental q_{eq} values were found to be smaller than q_{max} indicating that the biosorption of nickel(II) ions by inactivated *E. prolifera* is occurred by a monolayer type adsorption in which the surface of algae is not fully covered.

The experimental and calculated isotherms obtained from the studied isotherm models for the biosorption of nickel(II) ions on *E. prolifera* were given in Fig. 8. According to R^2 values in Table 3 and Fig. 8, the biosorption data of nickel(II) ions on *E. prolifera* fitted very well to both the Langmuir ant the Freundlich isotherm models. It is also observed from Table 3 that, the almost all calculated n_F values related to Freundlich isotherm are greater than unity representing favorable biosorption conditions. The maximum uptake capacity of *E. prolifera* for nickel(II) ions was also noted to be higher than the other previously reported biosorbents and adsorbents (Table 4). Differences of metal uptake are due to the properties of each adsorbent/biosorbent material such as structure, functional groups and surface area and solution chemistry.

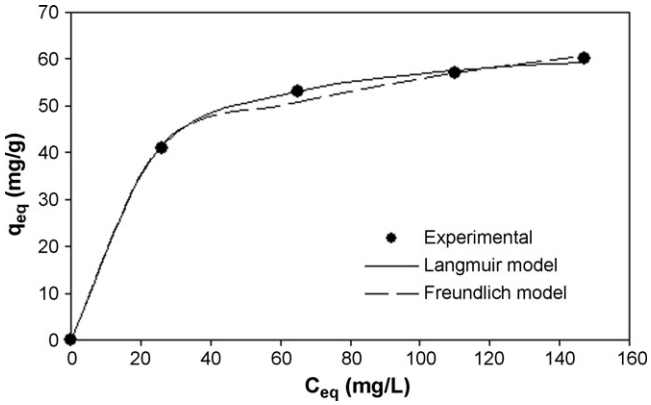

Fig. 8. The experimental and calculated isotherms (T: 30 °C; pH 5; X_o: 1.0 g/L; agitation rate: 100 rpm).

3.3. Kinetic study of nickel(II) biosorption

In order to examine the rate limiting step in the removal of nickel(II) ions by *E. prolifera*, the mass transfer and chemical reaction kinetics such as intraparticle diffusion model, external diffusion model and the pseudo second order kinetic model were used to test the experimental data of nickel(II) biosorption by *E. prolifera*.

3.3.1. The pseudo second order kinetic model

Information on the kinetics of metal uptake is required for selecting optimum operating conditions for full-scale batch metal removal processes [12]. The kinetics of nickel(II) biosorption on *E. prolifera* were tested using the pseudo second order kinetic model. The pseudo second order kinetic model is also based on the adsorption capacity of the solid phase [21]. This model predicts the behaviour over the whole range of adsorption and is in agreement with an adsorption mechanism being the rate-controlling step. In order to quantify the extent of uptake in adsorption kinetics, a pseudo second order kinetic model can be used. The linear form of the pseudo second order equation

Table 3
The Langmuir and Freundlich isotherm constants obtained from nickel(II) biosorption on *E. prolifera* at different temperatures and initial pH values

Temperature (°C)	q_{max} (mg/g)	b (L/mg)	R^2	K_F [(mg/g)(mg/L)$^{-1/n_F}$]	n_F	R^2
20	55.55	0.0461	0.9989	6.31	2.40	0.9987
25	58.82	0.0754	0.9941	14.31	3.86	0.9896
30	65.36	0.0663	0.9928	20.21	4.94	0.9941
Initial pH	q_{max} (mg/g)	b (L/mg)	R^2	K_F [(mg/g)(mg/L)$^{-1/n_F}$]	n_F	R^2
2.0	48.54	0.0805	0.9922	14.89	4.49	0.9984
3.0	52.91	0.0743	0.9957	16.20	4.56	0.9987
4.0	56.18	0.0832	0.9930	17.89	4.66	0.9973
5.0	65.36	0.0663	0.9928	20.21	4.94	0.9941

Table 4
The comparison of the monolayer coverage capacities of various adsorbents/biosorbents for nickel(II) ions

Adsorbent/biosorbent	q_{max} (mg/g)	References
Na-mordenite	5.324	[2]
Dye loaded sawdust	9.870	[16]
Peat	8.520	[21]
C. vulgaris	59.700	[22]
S. obliquus	30.200	[22]
Synechocystis sp.	189.800	[22]
Kaolinite	1.669	[23]
S. cerevisiae	46.300	[24]
Bagasse fly ash	6.490	[25]
Immobilized hybrid biosorbent (IHB)	101.140	[26]
Enteromorpha prolifera	65.360	This study

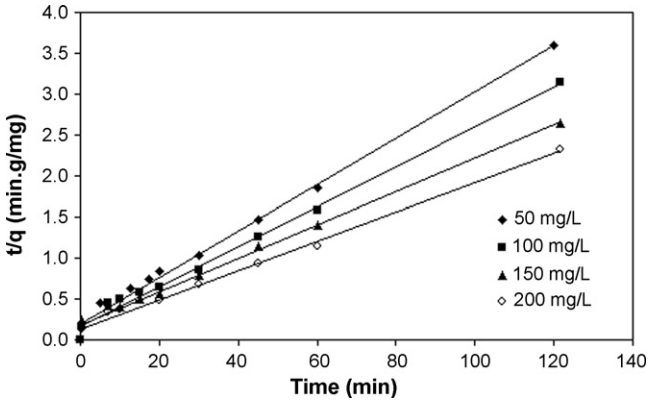

Fig. 9. The pseudo second order kinetic model plots at different nickel(II) ion concentrations (T: 30 °C; pH 5; X_o: 1.0 g/L; agitation rate: 100 rpm).

can be represented as [21]:

$$\frac{t}{q} = \frac{1}{k_2 q_{eq}^2} + \frac{t}{q_{eq}} \quad (8)$$

where k_2 is the rate constant of pseudo second order kinetic (g/mg min), q_{eq} and q are the biosorbed metal amount per unit weight of biosorbent at equilibrium and any time, t (min), respectively. If the pseudo second order kinetic model is applicable, the plot of t/q against t of Eq. (8) should give a linear relationship, from which calculated $q_{eq,cal}$ and k_2 can be determined from the slope and intercept of the plot.

Fig. 9 shows the plots of the linearized form of the pseudo second order kinetic model for the biosorption of nickel(II) ions on *E. prolifera* at 50, 100, 150 and 200 mg/L of the initial nickel(II) ion concentrations at 30 °C temperature and initial pH 5.0. Table 5 presents the k_2, regression cefficients, R^2, the experimental ($q_{eq,exp}$) and calculated ($q_{eq,cal}$) equilibrium uptake values for the different initial nickel(II) ion concentrations and temperatures. As shown in Table 5, the pseudo second order rate constants were affected by both the initial nickel(II) ion concentration and temperature. It was observed that the equilibrium nickel(II) biosorption capacity of *E. prolifera* increases with the increase in the initial nickel(II) ion concentration. Increasing the rate constants with increasing the nickel(II) ion concentration in solution seems to reduce the diffusion of solute in the boundary layer and to enhance the diffusion in the solid. Also, the experimental equilibrium data for nickel(II) ions are in good agreement with those calculated using the pseudo second order kinetics for the studied parameters. The regression coefficients obtained from the pseudo second order rate kinetic model were greater than 0.99 for all of the initial nickel(II) ion concentrations and temperatures. These confirm that the biosorption of nickel(II) ions on *E. prolifera* follows the pseudo second order kinetic model.

Table 5
The rate constants obtained from the pseudo second order kinetic model, the experimental and calculated equilibrium uptake amounts at different initial nickel(II) concentrations and temperatures

C_o (mg/L)	Temperature (°C)	$q_{eq,exp}$ (mg/g)	k_2 (g/mg min)	$q_{eq,cal}$ (mg/g)	R^2
50	20	28	0.0047	28.57	0.9908
100	20	35	0.0038	35.71	0.9919
150	20	44	0.0030	43.10	0.9905
200	20	52	0.0023	51.28	0.9906
50	25	31	0.0046	31.15	0.9922
100	25	36	0.0040	36.36	0.9920
150	25	46	0.0031	46.08	0.9906
200	25	55	0.0025	54.34	0.9922
50	30	35	0.0042	35.21	0.9930
100	30	40	0.0041	40.32	0.9922
150	30	49	0.0024	48.54	0.9911
200	30	56	0.0024	56.17	0.9902

3.3.2. Weber–Morris model (intraparticle diffusion) and boundary layer diffusion model

An emprically found functional relationship, common to the most adsorption processes, is that the uptake varies almost proportionally with $t^{1/2}$, the Weber–Morris plot, rather than with the contact time, t [27]:

$$q = K_i t^{1/2} \quad (9)$$

where q (mg/g) is the adsorbed metal amount, K_i intraparticle diffusion rate constant (mg/g min$^{1/2}$). According to this model, the plot of uptake (q) versus the square root of time should be linear if intraparticle diffusion is involved in the adsorption process and if these lines pass through the origin then intraparticle diffusion is the rate-controlling step. Previous studies showed that such plots may present a multi-linearity which indicates that two or more steps occur. The first, sharper portion is the external surface adsorption or instantaneous adsorption stage. The second portion is the gradual adsorption stage, where the intraparticle diffusion is rate-controlled. The third portion is final equilibrium stage where the intraparticle diffusion starts to slow down due to extremely low solute concentrations in the solution.

External mass transfer or boundary layer diffusion can be characterized by the initial rate of solute adsorption and can be described by the following equation [28]:

$$\left[\frac{d(C/C_o)}{dt}\right]_{t=0} = -\beta_L S \quad (10)$$

where β_L is the external mass transfer coefficient (cm/min), C is the solute concentration (mg/L), C_o is the initial solute concentration (mg/L) and S is the specific surface area for the mass transfer, with the assumption $C = C_o$ at $t = 0$ and external mass transfer coefficients were determined from the slopes as $t \to 0$.

Weber–Morris model and boundary layer diffusion model were applied to the biosorption of nickel(II) ions on *E. prolifera* as a function of initial metal ion concentration and the biosorbent concentration. Figs. 10 and 11 show the Weber–Morris model and boundary layer model plots obtained from the biosorption of nickel(II) ions on *E. prolifera* at different initial nickel(II) ion concentrations, respectively. Similar plots were also obtained for different biosorbent concentrations (data not shown). The parameters and regression coefficients obtained from the Weber–Morris and boundary layer diffusion model plots for nickel(II) biosorption were given in Table 6 for the

Table 6
Intraparticle diffusion and boundary layer model parameters

C_o (mg/L)	T (°C)	X_o (g/L)	$q_{eq,exp}$ (mg/g)	K_i (mg/g min$^{1/2}$)	R^2	$\beta_L S$ (1/min)	R^2
50	30	1.0	35.0	4.41	0.94	0.0228	0.96
100	30	1.0	40.0	6.49	0.96	0.0154	0.98
150	30	1.0	49.0	6.58	0.92	0.0118	0.98
200	30	1.0	56.0	7.24	0.91	0.0096	0.99
X_o (g/L)	T (°C)	C_o (mg/L)	$q_{eq,exp}$ (mg/g)	K_i (mg/g min$^{1/2}$)	R^2	$\beta_L S$ (1/min)	R^2
0.5	30	100	58.0	9.77	0.98	0.0097	0.98
1.0	30	100	40.0	6.49	0.96	0.0154	0.97
2.0	30	100	27.5	5.16	0.97	0.0190	0.98

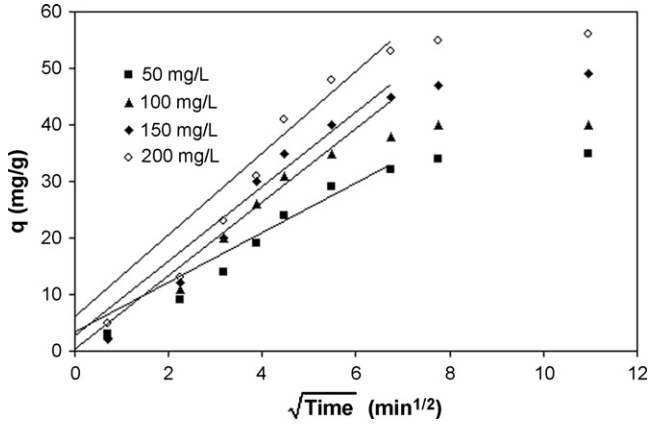

Fig. 10. Weber–Morris plots (T: 30 °C; pH 5; X_o: 1.0 g/L; agitation rate: 100 rpm).

studied initial metal ion concentrations and biosorbent concentrations. As can be seen from Table 6, the intraparticle diffusion rate constants (K_i) increased with initial nickel(II) ion concentration and decreased with biosorbent concentration. It was observed that the external mass transfer coefficients decreased with increasing the initial nickel(II) ion concentration and increased with increasing the biosorbent concentration. Higher $\beta_L S$ (1/min) values indicate the decrease of the external mass transfer resistance to nickel(II) biosorption.

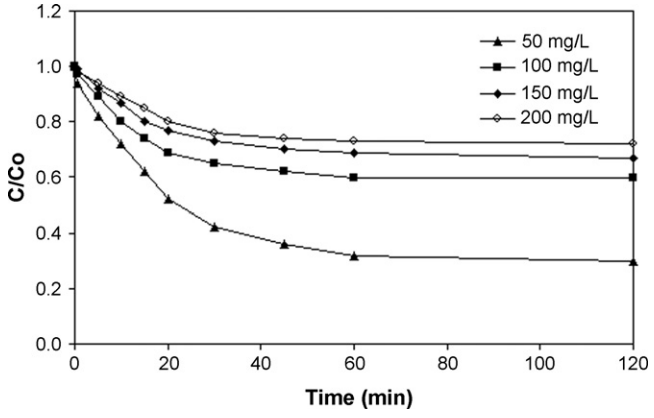

Fig. 11. Boundary layer model plots (T: 30 °C; pH 5; X_o: 1.0 g/L; agitation rate: 100 rpm).

4. Conclusion

The biosorption of nickel(II) ions on *E. prolifera*, a green algae, was investigated in a batch system. The biosorption conditions of nickel(II) ions on *E. prolifera* were optimized by using response surface methodology. The relationship between the responses and the independent variables was developed via the quadratic approximating functions of nickel(II) biosorption capacity of biosorbent and biosorption percent at the end of 120 min biosorption. The optimum biosorption conditions were determined as initial pH 4.3, temperature 27 °C, biosorbent concentration 1.2 g/L and initial nickel(II) concentration 100 mg/L. At optimum biosorption conditions, the uptake capacity of *E. prolifera* for nickel(II) ions was found as 36.8 mg/g while the biosorbed nickel(II) ion concentration was obtained as 44.2 mg/L after 120 min biosorption. The Langmuir and Freundlich isotherm models were applied to equilibrium data and defined very well both isotherm models. The monolayer coverage capacity of *E. prolifera* for nickel(II) ions was found as 65.66 mg/g. In order to examine the controlling mechanism of nickel(II) biosorption, the mass transfer models and chemical reaction kinetics such as intraparticle diffusion model, external diffusion model and the pseudo second order kinetic model were tested with the experimental data. As a result, a chemical waste such as nickel(II) ions can be removed by using a biological waste such as *E. prolifera* which is abundant and cheaply available in nature.

References

[1] J.W. Patterson, Industrial Wastewater Treatment Technology, second ed., Butterworth-Heinemann, Boston, 1985.
[2] X.S. Wang, J. Huang, H.Q. Hu, J. Wang, Y. Qin, Determination of kinetic and equilibrium parameters of the batch adsorption of nickel(II) from aqueous solutions by Na-mordenite, J. Hazard. Mater. 142 (2007), 468-467.
[3] M.H. Kalavathy, T. Karthikeyan, S. Rajgopal, L.R. Miranda, Kinetic and isotherm studies of Cu(II) adsorption onto H_3PO_4-activated rubber wood sawdust, J. Colloid. Interf. Sci. 292 (2005) 354–362.
[4] N. Akthar, S. Sastry, M. Mohan, Biosorption of silver ions by processed *Aspergillus niger* biomass, Biotechnol. Lett. 17 (1995) 551–556.
[5] S. Pradhan, S. Singh, L.C. Rai, Characterization of various functional groups present in the capsule of microcystis and study of their role in biosorption of Fe, Ni and Cr, Bioresour. Technol. 98 (2007) 595–601.
[6] Q. Yu, J.T. Matheickal, P. Yin, P. Kaewsarn, Heavy metal uptake capacities of common marine macro algal biomass, Water Res. 33 (1999) 1534–1537.

[7] Z.R. Holan, B. Volesky, Biosorption of lead and nickel by biomass of marine algae, Biotechnol. Bioeng. 43 (1994) 1001–1009.
[8] A. Özer, D. Özer, H.İ. Ekiz, Application of Freundlich and Langmuir models to multistage purification process to remove heavy metal ions by using *Schizomeris leibleinii*, Process Biochem. 34 (1999) 919–927.
[9] P. Kaewsarn, Biosorption of copper(II) from aqueous solutions by pretreated biomass of marine algae *Padina* sp., Chemosphere 47 (2002) 1081–1085.
[10] V.K. Gupta, A. Rastogi, V.K. Saini, N. Jain, Biosorption of copper(II) from aqueous solutions by *Spirogyra* species, J. Colloid. Interf. Sci. 296 (2006) 59–63.
[11] S. Karthikeyan, R. Balasubramanian, C.S.P. Iyer, Evaluation of the marine algae *Ulva fasciata* and *Sargassum* sp. for the biosorption of Cu(II) from aqueous solutions, Bioresour. Technol. 98 (2007) 452–455.
[12] M.A. Hashim, K.H. Chu, Biosorption of cadmium by brown, green and red seaweeds, Chem. Eng. J. 97 (2004) 249–255.
[13] D.C. Montgomery (Ed.), Design and Analysis of Experiments, fourth ed., John Wiley & Sons, New York, 1996.
[14] R.H. Myers, D.C. Montgomery, Response Surface Methodology: Process and Product Optimization using Designed Experiments, second ed., John Wiley & Sons, New York, 2002.
[15] G. Annadurai, R.S. Juang, D.J. Lee, Adsorption of heavy metals from water using banana and orange peels, Water Sci. Technol. 47 (2003) 185–190.
[16] S.R. Shukla, R.S. Pai, Adsorption of Cu(II), nickel(II) and Zn(II) on dye loaded groundnut shells and sawdust, Sep. Purif. Technol. 43 (2005) 1–8.
[17] H. Benaissa, M.A. Elouchdi, Removal of ions from aqueous solutions by dried sunflower leaves, Chem. Eng. Process. 46 (2007) 614–622.
[18] E.A. Oliveira, S.F. Montanher, A.D. Andrade, J.A. Nobrega, M.C. Rollemberg, Equilibrium studies for the sorption of chromium and nickel from aqueous solutions using raw rice bran, Process Biochem. 40 (2005) 3485–3490.
[19] I. Langmuir, J. Am. Soc. 40 (1918) 1361–1403.
[20] H.M.F. Freundlich, Über die adsorption in lösungen zeitschrift für Physikalische Chemie (Leipzig) 57A (1906) 385–470.
[21] Y.S. Ho, G. McKay, Pseudo second order model for sorption processes, Process Biochem. 34 (1999) 451–465.
[22] G.D. Çetinkaya, Z. Aksu, A. Öztürk, T. Kutsal, A comparative study on heavy metal biosorption characteristics of some algae, Process Biochem. 34 (1999) 885–892.
[23] Ö. Yavuz, Y. Altunkaynak, F. Güzel, Removal of, nickel, cobalt and manganese from aqueous solution by kaolinite, Water Res. 37 (2003) 948–952.
[24] A. Özer, D. Özer, Comparative study of the biosorption of Pb(II), nickel(II) and Cr(VI) ions onto *S. cerevisiae*. Determination of biosorption heats, J. Hazard. Mater. B100 (2003) 219–229.
[25] V.C. Srivastava, I.D. Mall, I.M. Mishra, Equilibrium modelling of single and binary adsorption of cadmium and nickel onto bagasse fly ash, Chem. Eng. J. 117 (2006) 79–91.
[26] M. Iqbal, A. Saeed, Production of an immobilized hybrid biosorbent for the sorption of Ni(II) from aqueous solution, Process Biochem. 42 (2007) 148–157.
[27] J.R. Weber, J.C. Morris, J. Sanit. Eng. Div. ASCE 89 (1963) 31–59.
[28] Y. Sağ, Y. Aktay, Kinetic studies on sorption of Cr(VI) and Cu(II) ions by chitin, chitosan and *Rhizopus arrhizus*, Biochem. Eng. J. 12 (2002) 143–153.